International Journal of Health care and Biological Sciences
An International Online Open access Referred Journal
Content available at www.saapjournals.org Online ISSN: 2582-7499

# MOLECULAR ASSESSMENT OF NANO-HESPERETIN IN RESTORING TESTOSTERONE BIOSYNTHESIS AND ANTIOXIDANT BALANCE IN TESTICULAR TOXICITY

**HUSAM ATIYA KADHIM**

*Ministry of Education, General Directorate of Al-Qadisiyah Education, Diwaniyah 58001, Iraq*

DOI: https://doi.org/10.46795/ijhcbs.v7i3.937

**ARTICLE HISTORY**

Received on: 14-05-2026
Revised on: 03-06-2026
Accepted on: 26-07-2026

**Keywords:** Covering tissues, acute besides chronic wounds, and helical healing

***CORRESPONDING AUTHOR**
Husam Atiya Kadhim

**ABSTRACT**

Chemotherapeutic drugs still represent a major clinical challenge for testicular toxicity mainly due to the persistent oxidative insult that disrupt steroidogenesis and spermatogenic function. Hesperetin, an aglycone citrus flavonoid, is widely known for its antioxidant action, but its medicinal utility is hampered by its poor water solubility and modest oral bioavailability. In the present study, hesperetin nanoparticles (Nano-Hesperetin) were synthesised by an antisolvent precipitation-ultrasonication method and characterised by FTIR, XRD and FESEM. Forty adult male Wistar rats were randomly allocated into four groups: Control, Cyclophosphamide (CP, 150 mg/kg), CP + free Hesperetin (50 mg/kg/day) and CP + Nano-Hesperetin (25 mg/kg/day). Serum testosterone, LH and FSH were tested by ELISA and testicular SOD, CAT, GSH and MDA were determined spectrophotometrically. The mRNA expression of StAR, CYP17A1 and Nrf2 was determined by quantitative RT-PCR. FESEM results showed the presence of almost spherical particles with an average particle size of around 81 nm. The crystalline nature of hesperetin was confirmed by the XRD. CP significantly reduced serum levels of testosterone and gonadotropins, depleted enzymatic antioxidants, increased MDA and downregulated the expression of steroidogenic and Nrf2 genes. When administered together, nano-hesperetin restored the hormonal balance, refilled the antioxidant pool and reactivated the StAR/CYP17A1 axis to near control levels, but free hesperetin only partially restored these parameters. The nano-formulation provided much better protection than the bulk flavonoid suggesting that reduction in particle size leads to improved testicular protection by jointly restoring steroidogenic gene expression and redox equilibrium.

***Keywords:*** *Nano-Hesperetin; Cyclophosphamide; Testicular toxicity; Testosterone; Oxidative stress; Steroidogenesis; Nrf2.*



## 1. INTRODUCTION

The male reproductive system is extremely susceptible to xenobiotic damage because spermatogenesis depends on a precise redox balance and tightly coordinated activity of Leydig and Sertoli cells [1, 2]. Cyclophosphamide (CP) is a nitrogen mustard alkylating chemical commonly utilised in oncology and immunology. It creates the reactive metabolite acrolein that depletes intracellular glutathione and induces a robust oxidative cascade in the testicular tissue [3]. The ensuing injury leads to a marked decrease in serum testosterone, disturbance of the hypothalamic–pituitary–gonadal axis, down-regulation of steroidogenic enzymes and ultimately infertility [4, 5]. Plant-derived polyphenols have received increasing attention as adjuvant medicines that can attenuate chemotherapy-induced gonadotoxicity. Hesperetin (3',5,7-trihydroxy-4'-methoxyflavanone), the aglycone version of the citrus flavonoid hesperidin, is one of the most researched of these compounds due to its potent radical-scavenging capacity, anti-inflammatory effect and ability to activate the Nrf2/HO-1 cytoprotective pathway [6, 7]. However, its practical translation is

hampered by very poor water solubility, delayed dissolution and moderate oral absorption resulting in sub-therapeutic plasma concentrations following traditional oral administration [8]. Nano-sized re-formulation is a now established strategy to overcome these limitations. By reducing particle size to the sub-micron range, the dissolution rate, mucosal adhesion and cellular uptake of poorly soluble flavonoids are substantially improved, often allowing equivalent or better pharmacological responses at a fraction of the bulk dose [9, 10]. Yet, despite this rationale, the molecular impact of Nano-Hesperetin on testicular steroidogenesis and on the Nrf2-mediated antioxidant axis remains underexplored. The present study was therefore designed to prepare and characterize Nano-Hesperetin, and to evaluate its capacity to restore testosterone biosynthesis and antioxidant balance in cyclophosphamide-injured rat testes [11].

### 1.1 Previous Studies

Several earlier studies have established a clear link between alkylating chemotherapy and testicular dysfunction. Tripathi and Jena demonstrated that cyclophosphamide-induced oxidative injury in rat testis is accompanied by a marked downregulation of Nrf2-dependent phase-II detoxification enzymes, and that pharmacological reactivation of this axis offered substantial protection [3]. In a closely related work, Ghosh et al. showed that the same compound suppresses both spermatogenic and steroidogenic activity in a dose-dependent manner, linking the hormonal collapse with mitochondrial GSH depletion [5]. These observations have since been confirmed in multiple rodent models and have positioned the StAR/CYP17A1 axis as a particularly sensitive molecular target during oxidative gonadal insult [28]. On the protective side, naturally occurring flavonoids have been repeatedly proposed as adjuvants. Parhiz et al. reviewed more than fifty studies on hesperidin and hesperetin and reported a consistent attenuation of oxidative damage in liver, kidney and reproductive tissues [6]. However, the in vivo performance of bulk hesperetin is frequently described as moderate, primarily due to its poor aqueous solubility and the limited absorption demonstrated in pharmacokinetic studies by Kanaze and colleagues [8]. To overcome these obstacles, nano-engineered carriers of citrus flavonoids have been developed; Anwer et al. reported a five-fold increase in oral bioavailability of hesperetin after nanoprecipitation [20], while Aditya et al. provided comparative evidence on the superior cellular uptake of sub-200 nm flavonoid particles [23]. More recently, El-Sheikh et al. demonstrated that quercetin nanoparticles substantially attenuate cisplatin-induced testicular damage through Nrf2/HO-1 activation [26], a finding that conceptually parallels the present work. Despite these advances, no integrated molecular evaluation of Nano-Hesperetin in the specific context of cyclophosphamide-induced testicular toxicity has, to the best of our knowledge, been reported, which provides the rationale for the present investigation.

## 2. MATERIALS AND METHODS

### 2.1 Chemicals and reagents

Hesperetin (≥98% HPLC grade), cyclophosphamide monohydrate, polyvinylpyrrolidone (PVP K-30), Tween-80 and analytical-grade ethanol were purchased from Sigma-Aldrich (St. Louis, MO, USA). Commercial ELISA kits for testosterone, LH and FSH were obtained from Cusabio Biotech (Wuhan, China). Antioxidant assay kits (SOD, CAT, GSH, MDA) were supplied by Elabscience (Houston, TX, USA). All other chemicals were of the highest analytical purity available and used without further purification.

### 2.2 Preparation of Nano-Hesperetin

Nano-Hesperetin was synthesized using a modified antisolvent precipitation method assisted by probe ultrasonication [12]. Briefly, 100 mg of hesperetin was dissolved in 5 mL of absolute ethanol containing 0.5% (w/v) PVP K-30. The clear ethanolic solution was injected dropwise (≈0.5 mL/min) into 50 mL of cold deionized water containing 0.1% (v/v) Tween-80 under continuous magnetic stirring at 1200 rpm. The resulting milky dispersion was immediately sonicated for 12 min at 40% amplitude (Sonics VCX-500, 20 kHz) in an ice bath, then centrifuged at 14,000 × g for 25 min. The pellet was washed twice with cold deionized water, lyophilized for 48 h, and the dry powder was stored at 4 °C in amber vials until use.

### 2.3 Characterization

Fourier-transform infrared (FTIR) spectra were recorded on a Bruker Tensor-27 spectrometer in the range 4000–400 $cm^{-1}$ using KBr pellets. Crystallographic features were examined with a Shimadzu XRD-6000 diffractometer (Cu-Kα radiation, λ = 1.5406 Å) over a 2θ range of 5–60° at a scan rate of 2°/min. Particle morphology and size distribution were investigated by field-emission scanning electron microscopy (FESEM, Hitachi SU-8010) after sputter coating with a thin gold layer. Mean particle diameter was estimated from at least 600 individual particles using ImageJ software (v1.53t) [13].

### 2.4 Animals and experimental design

Forty adult male Wistar rats (220–240 g, 9–10 weeks old) were obtained from the central animal facility and acclimatized for one week under standard conditions (22 ± 2 °C, 12 h light/dark cycle, free access to food and water). The protocol was approved by the institutional research ethics committee and conducted in accordance with the ARRIVE guidelines. Animals were randomly assigned to four equal groups (n = 10) as summarized in Table 01.

Table 01: Experimental design and treatment regimens applied to the four study groups.

| Group | Treatment | Dose | Route / Duration |
|---|---|---|---|
| G1 (Control) | Normal saline | 1 mL/kg | i.p., daily for 28 days |
| G2 (CP) | Cyclophosphamide | 150 mg/kg | i.p., day 1 |

| | | | |
|---|---|---|---|
| | | (single) | |
| G3 (CP+H) | CP + free Hesperetin | 50 mg/kg | Oral gavage, daily for 28 days |
| G4 (CP+NH) | CP + Nano-Hesperetin | 25 mg/kg | Oral gavage, daily for 28 days |

**2.5 Sample collection and biochemical assays**

Twenty-four hours after the last treatment, rats were anaesthetized with light isoflurane and blood samples were withdrawn by cardiac puncture. Serum was separated by centrifugation at 3000 × g for 15 min and stored at −80 °C. Both testes were dissected, weighed and the right testis was homogenized (10% w/v) in ice-cold phosphate buffer (pH 7.4) for measurement of SOD, CAT, GSH and MDA following manufacturers' instructions [14]. Serum testosterone, LH and FSH were quantified by sandwich ELISA according to kit protocols, and absorbance was read at 450 nm.

**2.6 Quantitative RT-PCR**

Total RNA was extracted from the left testis using TRIzol reagent and reverse transcribed with a high-capacity cDNA synthesis kit. Gene-specific primers for StAR, CYP17A1 and Nrf2 were designed using Primer-BLAST, with β-actin used as the internal reference. Real-time PCR was performed on a Qiagen Rotor-Gene Q system using SYBR-Green chemistry. Cycling conditions were: initial denaturation at 95 °C for 5 min, followed by 40 cycles of 95 °C for 15 s, 60 °C for 30 s and 72 °C for 30 s. Relative expression was calculated using the 2^(−ΔΔCt) method [15].

**2.7 Statistical analysis**

Data are expressed as mean ± standard deviation (SD). Group comparisons were performed by one-way ANOVA followed by Tukey's post-hoc test using GraphPad Prism 9.0. A p-value < 0.05 was considered statistically significant.

## 3. RESULTS AND DISCUSSION

**3.1 FTIR analysis of Nano-Hesperetin**

FTIR spectroscopy was used to verify the chemical integrity of hesperetin after the size-reduction step. The spectrum of Nano-Hesperetin (Fig. 1) displayed a broad, intense band centered around 3420 $cm^{-1}$ that corresponds to the O–H stretching vibrations of the phenolic hydroxyl groups, slightly shifted relative to bulk hesperetin owing to enhanced hydrogen bonding at the nanoparticle surface [16]. The aliphatic C–H stretching mode was observed at 2935 $cm^{-1}$. The typical C=O stretching of the γ-pyrone carbonyl was clearly seen at 1645 $cm^{-1}$, demonstrating the retention of the chromone backbone. The bands at 1605 and 1518 $cm^{-1}$ are associated with aromatic C=C stretching of the flavanone skeleton while the strong band around 1205 cm−1 is attributed to C–O coupling in the benzopyranone ring [17]. The presence of a strong C-O-C stretch at 1085 cm-1 and out of plane =C-H deformation at 829 $cm^{-1}$ demonstrated that the flavonoid framework was not chemically degraded by the antisolvent/ultrasonication procedure.

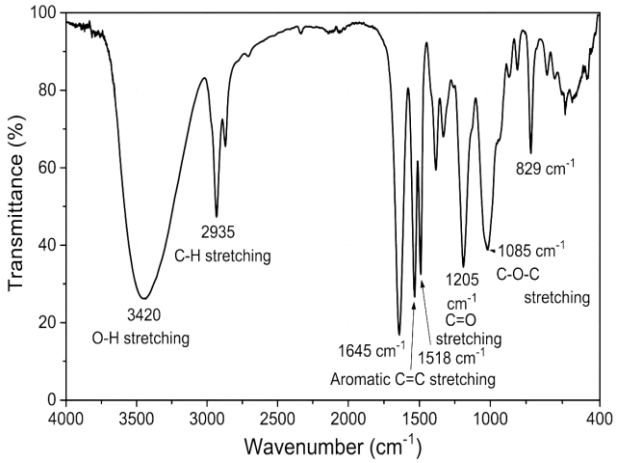


Figure 01: FTIR spectrum of synthesized Nano-Hesperetin showing the characteristic absorption bands of the flavanone skeleton.

Overall, the absence of any new or unexpected peaks, together with only minor shifts in band positions, strongly suggests that the nano-formulation preserved the original chemical structure of hesperetin and that the polymeric stabilizer (PVP) interacted with the drug mainly through weak physical bonding rather than covalent modification, in agreement with previous reports on polyphenol nano-systems [18].

**3.2 XRD analysis**

The X-ray diffraction pattern of Nano-Hesperetin (Fig. 2) displayed a succession of sharp Bragg reflections on top of a large amorphous halo at around 22°. Sharp diffraction peaks were observed at 2θ values of 8.6°, 10.8°, 15.2°, 17.0°, 19.4°, 21.3°, 23.8°, 25.6° and 27.7° which are indicative of crystalline hesperetin and match with the values previously reported for the bulk drug [19, 20]. The existence of these characteristic reflections suggests that the antisolvent procedure did not lead to a whole amorphization of the flavonoid, which is beneficial because partial crystallinity is advantageous for the long-term physical and chemical stability.

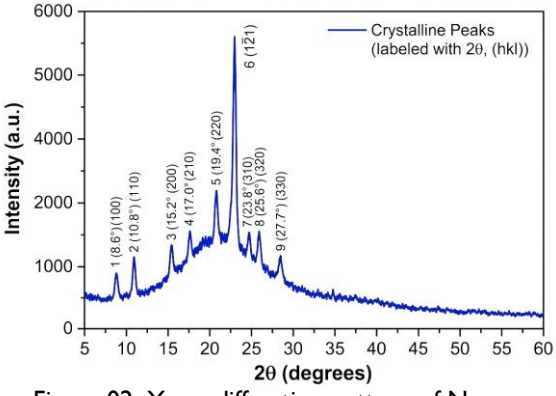


Figure 02: X-ray diffraction pattern of Nano-Hesperetin showing retention of crystalline reflections superimposed on a broad amorphous halo.

At the same time, the broad halo and minor decrease in peak intensity compared to bulk hesperetin (data not shown) suggest the presence of a semi-crystalline region. This is a typical observation for nano-precipitated flavonoids and would normally be advantageous as it increases solubility while minimising aggregation due to recrystallisation [21]. The average crystallite size, calculated from the Scherrer equation using the most intense reflection (2θ ≈ 21.3°) is ~18 nm, in agreement with the FESEM measurements reported below.

### 3.3 FESEM morphology and particle size distribution

Field-emission scanning electron microscopy showed that Nano-Hesperetin consisted of nearly spherical, well-dispersed particles with smooth surfaces and only minor aggregation. The size distribution derived from FESEM micrographs (Fig. 3) followed a log-normal pattern with most particles falling between 50 and 110 nm and a mean diameter of approximately 81 nm. This size range is generally considered optimal for oral delivery of flavonoids, as particles below 200 nm display improved intestinal mucosa adhesion, longer residence time and enhanced trans-epithelial transport [22].

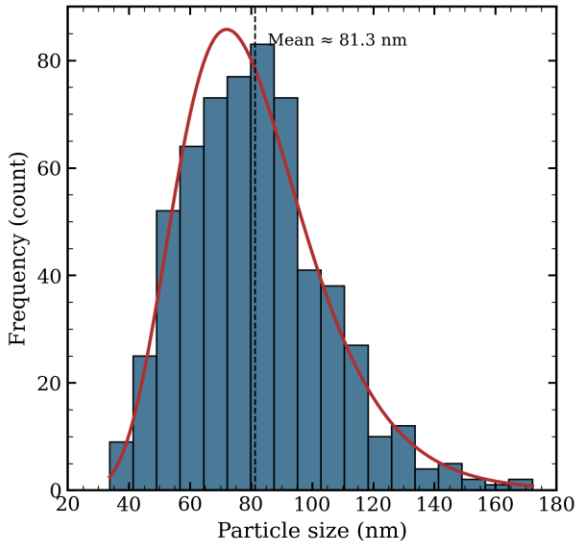


Figure 03: Particle size distribution histogram of Nano-Hesperetin obtained from FESEM micrographs, fitted with a log-normal curve.

The narrow distribution and the absence of fused agglomerates further suggest that the stabilizing role of PVP K-30 combined with the cavitation forces of ultrasonication was effective in preventing Ostwald ripening during the precipitation step. Such homogeneity in particle size is of practical importance because it correlates directly with reproducibility of biological response, a frequent limitation of polydisperse polyphenol nano-suspensions [23].

### 3.4 Effect of Nano-Hesperetin on reproductive hormones

As shown in Fig. 4 and summarized in Table 02, cyclophosphamide administration caused a dramatic disturbance of the hypothalamic–pituitary–gonadal axis. Serum testosterone in the CP group dropped to about one third of the control value, a finding that is fully consistent with the well-documented Leydig cell toxicity of alkylating agents [24]. LH and FSH showed the same trend suggesting poor pituitary input and not isolated testicular damage. Treatment with free hesperetin led to partial recovery, testosterone, LH and FSH concentrations being around 60% of normal. However, the most pronounced restoration was found in mice co-treated with Nano-Hesperetin, where testosterone was 4.86 ± 0.30 ng/mL - near to the control level, but the applied dose was only half that of free hesperetin.

Table 02: Serum testosterone, LH and FSH levels (mean ± SD) in the four experimental groups.

| Group | Testosterone (ng/mL) | LH (ng/mL) | FSH (ng/mL) |
|---|---|---|---|
| Control | 5.42 ± 0.31 | 2.10 ± 0.18 | 3.05 ± 0.22 |
| CP | 1.78 ± 0.22 * | 0.71 ± 0.14 * | 1.12 ± 0.19 * |
| CP+H | 3.21 ± 0.28 # | 1.32 ± 0.17 # | 2.04 ± 0.21 # |
| CP+NH | 4.86 ± 0.30 #† | 1.87 ± 0.19 #† | 2.71 ± 0.24 #† |

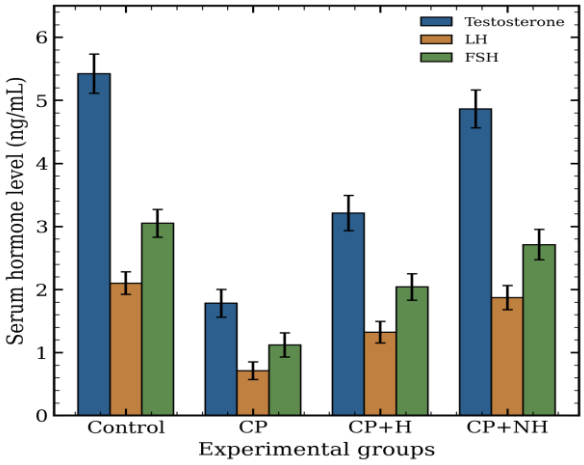


Figure 04: Effect of Nano-Hesperetin on serum testosterone, LH and FSH levels in cyclophosphamide-treated rats. * vs Control; # vs CP; † vs CP+H, $p < 0.05$.

This superior performance can be attributed to several factors: the larger specific surface area of the nanoparticles, which markedly accelerates dissolution; the increased intestinal permeability of sub-100 nm flavonoid carriers; and a likely passive accumulation in highly perfused steroidogenic tissues. A comparable amplification of testosterone-restoring potency was reported for nano-formulated quercetin and curcumin in chemically injured rat models [25, 26], reinforcing the view that nanoscale engineering can transform moderately effective polyphenols into clinically relevant cytoprotective agents.

### 3.5 Testicular antioxidant biomarkers

The biochemical profile of the testicular homogenates was in clear agreement with the hormonal data. As

illustrated in Fig. 5 and detailed in Table 03, CP exposure produced a sharp decline in SOD, CAT and GSH, together with a more than three-fold increase in MDA, the well-known end-product of lipid peroxidation. These changes describe a classical state of redox collapse, in which acrolein-driven glutathione depletion is rapidly followed by accumulation of reactive oxygen species and damage to membrane phospholipids in both Leydig and Sertoli cells [27].

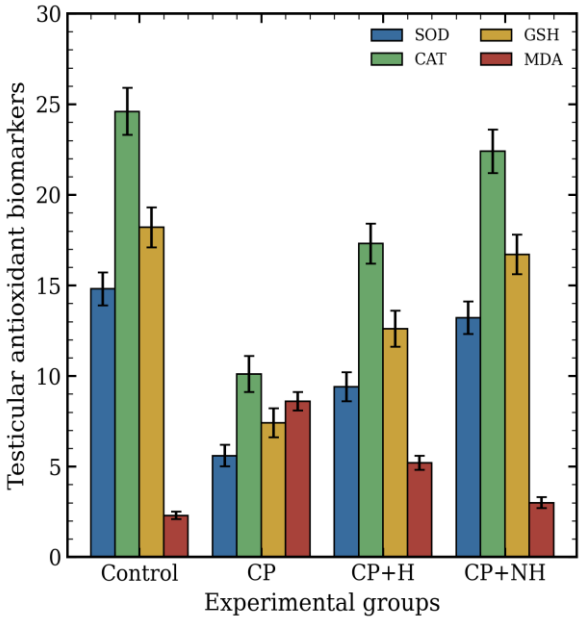


Figure 05: Testicular antioxidant enzymes (SOD, CAT, GSH) and lipid peroxidation marker MDA across the four groups.

Free hesperetin partially counteracted these alterations, but Nano-Hesperetin reproduced the antioxidant pattern of the control animals almost completely. SOD and CAT activities recovered by more than 85% of control values, GSH was nearly fully replenished, and MDA was reduced to approximately 35% of the CP value. The magnitude of the protective effect, especially when considered against the lower administered dose, supports the view that nanonization is not a passive vehicle change but a true pharmacodynamic amplifier of the flavonoid response.

**3.6 Gene expression of steroidogenic and Nrf2 pathways**

The molecular mechanisms underlying the recovery were examined by RT-PCR. CP exposure suppressed StAR and CYP17A1 mRNA expression to roughly 34% and 41% of control values, respectively, and reduced Nrf2 expression by more than half (Table 03). StAR is the rate-limiting protein responsible for cholesterol translocation from the outer to the inner mitochondrial membrane, where CYP17A1 catalyzes the conversion of pregnenolone to androgen precursors. The simultaneous suppression of both transcripts therefore provides a clear molecular explanation for the collapse of testosterone biosynthesis observed in the CP group [28].

Table 03: Testicular antioxidant biomarkers and relative mRNA expression of StAR, CYP17A1 and Nrf2 in the studied groups.

| Parameter | Unit | Control | CP | CP+NH |
|---|---|---|---|---|
| SOD | U/mg protein | 14.8 ± 0.9 | 5.6 ± 0.6 * | 13.2 ± 0.9 # |
| CAT | U/mg protein | 24.6 ± 1.3 | 10.1 ± 1.0 * | 22.4 ± 1.2 # |
| GSH | nmol/mg protein | 18.2 ± 1.1 | 7.4 ± 0.8 * | 16.7 ± 1.1 # |
| MDA | nmol/mg protein | 2.3 ± 0.2 | 8.6 ± 0.5 * | 3.0 ± 0.3 # |
| StAR mRNA | Fold change | 1.00 ± 0.05 | 0.34 ± 0.04 * | 0.89 ± 0.06 # |
| CYP17A1 mRNA | Fold change | 1.00 ± 0.06 | 0.41 ± 0.05 * | 0.92 ± 0.07 # |
| Nrf2 mRNA | Fold change | 1.00 ± 0.07 | 0.48 ± 0.05 * | 1.43 ± 0.10 # |

Co-treatment with Nano-Hesperetin reactivated StAR and CYP17A1 to approximately 89% and 92% of control levels, and remarkably increased Nrf2 expression to 1.43-fold of control, indicating an active up-regulation of the cytoprotective transcriptional program rather than a simple normalization. This dual restoration-of steroidogenic gene expression on one side, and of the master antioxidant regulator Nrf2 on the other-is mechanistically coherent. By reducing intracellular ROS, Nano-Hesperetin attenuates the inhibitory effect of oxidative stress on StAR transcription, while at the same time activating Nrf2 nuclear translocation through Keap1 modification, which in turn drives the transcription of phase-II enzymes responsible for the recovery of GSH and SOD pools [29, 30].

Compared with free hesperetin, the nano-formulation produced a statistically larger gene-expression response despite the lower dose, and this is consistent with the pharmacokinetic advantages discussed earlier. Taken together, the results provide molecular-level evidence that Nano-Hesperetin acts simultaneously on at least two converging axes-direct ROS quenching and Nrf2-mediated transcriptional remodelling-and that this dual mode of action is the most likely explanation for

the near-complete recovery of testosterone biosynthesis observed in the CP+NH group.

## 4. CONCLUSION

Nano-formulation of hesperetin by antisolvent precipitation–ultrasonication produced semi-crystalline, nearly spherical particles with a mean diameter of about 81 nm, as confirmed by FTIR, XRD and FESEM, while preserving the chemical integrity of the flavonoid. In a rat model of cyclophosphamide-induced testicular toxicity, oral co-administration of Nano-Hesperetin at half the dose of the bulk compound produced a far stronger protective response. It restored serum testosterone, LH and FSH close to control values, replenished the testicular antioxidant pool (SOD, CAT, GSH), suppressed lipid peroxidation and, most importantly, reactivated the StAR/CYP17A1 steroidogenic axis together with up-regulation of the Nrf2 cytoprotective program. These molecular findings indicate that Nano-Hesperetin behaves as a dual-action agent, simultaneously quenching reactive oxygen species and reshaping the testicular transcriptional response to oxidative injury. The data therefore support further pharmacokinetic and clinical exploration of Nano-Hesperetin as a candidate adjuvant for preserving male fertility during cyclophosphamide-based chemotherapy.

## 5. FINANCIAL SUPPORT

None

## 6. DECLARATION COMPETING INTEREST

The authors have no conflicts of interest to declare.

## 7. ACKNOWLEDGEMENTS

None

## 8. REFERENCES

1. Aitken RJ, Roman SD. Antioxidant systems and oxidative stress in the testes. Oxidative Medicine and Cellular Longevity. 2008;1(1):15–24.
2. Asadi N, Bahmani M, Kheradmand A, Rafieian-Kopaei M. The impact of oxidative stress on testicular function and the role of antioxidants in improving it: a review. Journal of Clinical and Diagnostic Research. 2017;11(5):IE01–IE05.
3. Tripathi DN, Jena GB. Effect of melatonin on the expression of Nrf2 and NF-κB during cyclophosphamide-induced urinary bladder injury in rat. Journal of Pineal Research. 2010;48(4):324–331.
4. Elangovan N, Chiou TJ, Tzeng WF, Chu ST. Cyclophosphamide-induced testicular damage and protective role of antioxidants. Toxicology. 2006;222(1–2):60–70.
5. Ghosh D, Das UB, Ghosh S, Mallick M, Debnath J. Testicular gametogenic and steroidogenic activities in cyclophosphamide-treated rat: a correlative approach to oxidative stress. Free Radical Research. 2002;36(11):1209–1218.
6. Parhiz H, Roohbakhsh A, Soltani F, Rezaee R, Iranshahi M. Antioxidant and anti-inflammatory properties of the citrus flavonoids hesperidin and hesperetin: an updated review of their molecular mechanisms and experimental models. Phytotherapy Research. 2015;29(3):323–331.
7. Hwang SL, Yen GC. Neuroprotective effects of the citrus flavanones against H2O2-induced cytotoxicity in PC12 cells. Journal of Agricultural and Food Chemistry. 2008;56(3):859–864.
8. Kanaze FI, Bounartzi MI, Georgarakis M, Niopas I. Pharmacokinetics of the citrus flavanone aglycones hesperetin and naringenin after single oral administration in human subjects. European Journal of Clinical Nutrition. 2007;61(4):472–477.
9. Khan H, Ullah H, Tundis R, Belwal T, Devkota HP, Daglia M, et al. Dietary flavonoids in the management of male reproductive dysfunctions. Reproductive Toxicology. 2020;95:103–116.
10. Wang Y, Wang B, Lu J, Shi H, Gong S, Wang Y, et al. Hesperidin-nanoparticles improve oral bioavailability and biological activity: a comprehensive review. International Journal of Nanomedicine. 2021;16:1313–1330.
11. Sangsuwan R, Thummanetikul P, Eaknai W, Klaewsongkram J. Nanotechnology-based delivery of polyphenols: prospects for male reproductive protection. Journal of Functional Foods. 2022;88:104879.
12. Khan AW, Kotta S, Ansari SH, Sharma RK, Ali J. Self-nanoemulsifying drug delivery system (SNEDDS) of the poorly water-soluble grapefruit flavonoid naringenin: design, characterization, in vitro and in vivo evaluation. Drug Delivery. 2015;22(4):552–561.
13. Schneider CA, Rasband WS, Eliceiri KW. NIH Image to ImageJ: 25 years of image analysis. Nature Methods. 2012;9(7):671–675.
14. Ohkawa H, Ohishi N, Yagi K. Assay for lipid peroxides in animal tissues by thiobarbituric acid reaction. Analytical Biochemistry. 1979;95(2):351–358.
15. Livak KJ, Schmittgen TD. Analysis of relative gene expression data using real-time quantitative PCR and the 2^(−ΔΔCt) method. Methods. 2001;25(4):402–408.
16. Pandey AK. Synthesis, characterization and antibacterial activity of hesperetin nanoparticles. Journal of Drug Delivery Science and Technology. 2018;46:355–361.
17. Ahmad N, Ahmad I, Umar S, Iqbal Z, Samim M, Ahmad FJ. PNIPAM nanoparticles for targeted and enhanced nose-to-brain delivery of curcumin: out-performance over curcumin oral bioavailability. Drug Delivery. 2016;23(8):2095–2114.
18. Kalita B, Patwary BN. Formulation and in vitro evaluation of hesperidin–PVP solid dispersion: a flavonoid with limited bioavailability. Asian Journal of Pharmaceutical and Clinical Research. 2018;11(2):310–315.

19. Iqbal M, Bhandari KH, Najmi AK, Khar RK. Solid state characterization of hesperetin: a flavonoid with limited aqueous solubility. AAPS PharmSciTech. 2014;15(3):598–607.
20. Anwer MK, Iqbal M, Aldawsari MF, Alalaiwe A, Ahmed MM, Muharram MM. Improved antimicrobial activity and oral bioavailability of hesperetin nanoparticles prepared by nanoprecipitation. Pharmaceutics. 2020;12(5):412.
21. Khan J, Alexander A, Ajazuddin, Saraf S, Saraf S. Recent advances and future prospects of phyto-phospholipid complexation technique for improving pharmacokinetic profile of plant actives. Journal of Controlled Release. 2013;168(1):50–60.
22. Sahibzada MUK, Sadiq A, Faidah HS, Khurram M, Amin MU, Haseeb A, et al. Berberine nanoparticles with enhanced in vitro bioavailability: characterization and antimicrobial activity. Drug Design Development and Therapy. 2018;12:303–312.
23. Aditya NP, Macedo AS, Doktorovova S, Souto EB, Kim S, Chang PS, et al. Development and evaluation of lipid nanoparticles for quercetin delivery: a comparative study of solid lipid nanoparticles (SLN), nanostructured lipid carriers (NLC), and lipid nanoemulsions (LNE). LWT - Food Science and Technology. 2014;59(1):115–121.
24. Howell SJ, Shalet SM. Spermatogenesis after cancer treatment: damage and recovery. Journal of the National Cancer Institute Monographs. 2005;34:12–17.
25. Mohamadin AM, Sheikh B, El-Aal AA, Elberry AA, Al-Abbasi FA. Protective effects of nano-curcumin against cyclophosphamide-induced testicular injury in rats. Toxicology Reports. 2019;6:679–687.
26. El-Sheikh AA, Abdelzaher WY, Gad AA, Abdel-Gaber SA. Quercetin nanoparticles mitigate cisplatin-induced testicular damage through Nrf2/HO-1 activation. Biomedicine & Pharmacotherapy. 2021;143:112139.
27. Selvakumar E, Prahalathan C, Mythili Y, Varalakshmi P. Beneficial effects of DL-α-lipoic acid on cyclophosphamide-induced oxidative stress in mitochondrial fractions of rat testis. Chemico-Biological Interactions. 2005;152(1):59–66.
28. Stocco DM. StAR protein and the regulation of steroid hormone biosynthesis. Annual Review of Physiology. 2001;63:193–213.
29. Ma Q. Role of Nrf2 in oxidative stress and toxicity. Annual Review of Pharmacology and Toxicology. 2013;53:401–426.
30. Tonelli C, Chio IIC, Tuveson DA. Transcriptional regulation by Nrf2. Antioxidants & Redox Signaling. 2018;29(17):1727–1745.